Reproduction of Ground Magnetic Variations During the SC and the Substorm From the Global Simulation and Biot - Savart's Law

Tanaka, T.; Ebihara, Y.; Watanabe, M.; Den, M.; Fujita, S.; Kikuchi, T.; Hashimoto, K. K.; Kataoka, R.

AGU100 ADVANCING EARTH AND SPACE SCIENCE

JGR Space Physics

RESEARCH ARTICLE
10.1029/2019JA027172

Key Points:
- Ground magnetic variations in the SC and the substorm are decomposed to four components by the simulation and Biot-Savart's law
- Fukushima's theorem is violated for the equatorial PRI, the AU/AL indices, and the positive bay of the substorm
- The conductivity model of the global simulation is verified by comparisons between reproduced and observed ground magnetic variations

Supporting Information:
- Supporting Information S1
- Movie S1
- Figure S1

Correspondence to:
T. Tanaka,
tatanaka@serc.kyushu-u.ac.jp

Citation:
Tanaka, T., Ebihara, Y., Watanabe, M., Den, M., Fujita, S., Kikuchi, T., et al. (2020). Reproduction of ground magnetic variations during the SC and the substorm from the global simulation and Biot-Savart's law. *Journal of Geophysical Research: Space Physics*, *125*, e2019JA027172. https://doi.org/10.1029/2019JA027172

Received 18 JUL 2019
Accepted 7 JAN 2020
Accepted article online 29 JAN 2020

Reproduction of Ground Magnetic Variations During the SC and the Substorm From the Global Simulation and Biot-Savart's Law

T. Tanaka[1], Y. Ebihara[2], M. Watanabe[1], M. Den[3], S. Fujita[4,7], T. Kikuchi[5], K. K. Hashimoto[6], and R. Kataoka[7]

[1]International Center for Space Weather Science and Education, Kyushu University, Fukuoka, Japan, [2]Research Institute for Sustainable Humanosphere, Kyoto University, Uji, Japan, [3]Space Environment Laboratory, National Institute of Information and Communications Technology, Tokyo, Japan, [4]Meteorological College, Kashiwa, Japan, [5]Institute of Space-Earth Environmental Research, Nagoya University, Nagoya, Japan, [6]Department of Agriculture, Kibi International University, Minamiawaji, Japan, [7]Space and Upper Atmospheric Group, National Institute of Polar Research, Tachikawa, Japan

Abstract In this paper, currents causing the sudden commencement (SC), the AU/AL indices, and the positive bay during the substorm are identified from the global simulation and Biot-Savart's law. Candidate currents assumed as causes of these ground magnetic variations are the ionospheric Hall current, the ionospheric Pedersen current, the field-aligned current (FAC), and other magnetospheric currents than the FAC. In general, FAC effect and Pedersen current effect cancel out each other under the restriction of Fukushima's theorem. During the SC, for instance, the midlatitude preliminary positive impulse appears in the prenoon and midlatitude preliminary reverse impulse (PRI) appears in the postnoon, due to the remaining effect of the Hall current. However, violations of the Fukushima's theorem are also common such as in the cases of the equatorial PRI, the auroral electrojet, and the positive bay. The equatorial PRI caused by the Pedersen current appears both in the prenoon and postnoon regions. In the auroral region, the Hall current effect prevails over other currents so much and determines the AU/AL indices only from it regardless other currents. The midlatitude positive bay on the nightside is generated by the effect of the FAC. From these diverse reproduction of ground magnetic variations, a further verification is given for the global simulation in reproductions of the magnetosphere-ionosphere coupling process.

1. Introduction

In recent years, various magnetospheric and ionospheric disturbances are reproduced realistically from high-resolution global simulations. These results are characterized by the reproduction of ionospheric variations simultaneously with corresponding magnetospheric structures. Such simulation result must be verified through the comparison with observations. In the course of comparison, however, it is difficult to compare calculated and observed magnetospheric structures globally, due to a lack of observational points. The main verification criterion for this comparison may be the time series, but a large error will occur even if there is a slight deviation in the location. On the other hand, a large number of observational stations are distributed world-widely for the ionosphere. By adopting these observations, simulation results have been validated through the global comparison of two-dimensional structures. Especially, it is possible to compare dynamical structures globally from the aurora, since the aurora can be observed as the time evolution of two-dimensional structures. Two-dimensional comparison is severer constraint than time series comparison. Through such comparison, we can obtain confirmation for the credibility of numerical solutions. In the simulation, there still remains a big uncertainty about how to determine ionospheric electric conductivity.

1.1. Auroral Reproduction

The global simulation reproduces a series of auroral phenomena during the substorm, such as the quiet arc (Tanaka, 2015; Tanaka, Ebihara, et al., 2019) and the preonset N-S arc (Ebihara & Tanaka, 2016) during the growth phase, the initial brightening at the onset (Ebihara & Tanaka, 2015a; Tanaka, Ebihara, et al., 2017; Tanaka, Ebihara, et al., 2019), and the westward traveling surge (WTS) during the expansion phase

(Ebihara & Tanaka, 2015b). The global simulation is verified by comparing these results with observations. It was discovered from these studies that the quiet arc is projection of convective shear on the plasma sheet-lobe boundary (Tanaka, Ebihara, et al., 2017), that the preonset N-S arc is a structure in the lobe (Ebihara & Tanaka, 2016), and that the onset is due to the formation of the near-earth dynamo (Ebihara & Tanaka, 2015a). Ebihara and Tanaka (2015b) have proposed a highly reliable mechanism (ionospheric polarization) of the WTS based on calculation results.

For such comparison in the ionosphere, validity of the global simulation has been confirmed also under the northward interplanetary magnetic field (IMF), in reproducing the Sun-aligned arc (Tanaka, Obara, et al., 2017), the theta aurora (Tanaka et al., 2004, 2018), and the fan-shaped arc (Tanaka, Obara, et al., 2019). These phenomena have been known for a long time, but consideration for their causes have been staying at the level of estimation. Global simulations have shown that these events are not the manifestation of local instability or structural deformation, but the projection of the topological structure of the entire magnetosphere. Above all, the conclusion that the theta aurora is the projection of the null replacing process adds another point of view to the magnetospheric physics. It adds another useful approach "topology" to the research of magnetosphere physics, which has been understood so far by the dynamics alone.

1.2. Magnetic Field Variations

In these comparisons between the global simulation and the aurora observation, the correspondence is considered under the assumption that upward field-aligned current (FAC) will generate aurora arcs. Under such assumption, solutions of the global simulation are effectively evaluated from auroras, and solutions verified in this way can reveal various mechanisms for each disturbance. Observations of ground magnetic field provide much more data for the comparison between the simulation and the observation. These observations have been obtained for many categories over wide areas from high latitudes to low latitudes. Magnetic variations are classified to many categories from their characteristic appearances in space and time. Global simulations may not reach the level to reproduce individual variations perfectly, but at least it is possible to reproduce qualitative appearances of each magnetic field variations (Yu & Ridley, 2008). It is the purpose of the present paper to further develop this possibility.

Ground magnetic field variations have two main origins, one caused by the atmospheric motion and the other caused by the dynamics of the magnetosphere-ionosphere coupling system. Among them, variations reflecting the dynamics of the magnetosphere-ionosphere coupling system include effects of the ionospheric Hall current, the ionospheric Pedersen current, the FAC, and the magnetospheric current (the Chapman-Ferraro (CF) current + the cusp current + the tail current + the ring current) (Yu et al., 2010). This paper deals with these four components resulting from the dynamics of the magnetosphere-ionosphere coupling system. Under transient conditions such as the sudden commencement (SC) and the substorm onset, each component tends to prevail at different timing and different location. This paper treats the moderate substorm where the IMF Bz is above -5 nT and a strong ring current is absent, because the magnetohydrodynamics (MHD) solution is accurate in this range. By classifying ground magnetic variations from differences in contributing components, occurrence timing, and occurrence location, we can estimate corresponding disturbance mechanisms in the magnetosphere-ionosphere coupling system (Kikuchi et al., 2001).

The ionospheric Hall current, the ionospheric Pedersen current, the FAC, and the magnetospheric current (the CF current, the cusp current, and the tail current) are all obtained from the global simulation. The cause of magnetic field variation is studied for each category from simulation results by investigating how these four components act their individual roles depending on the type of magnetic field variation. Seen from the opposite side, these investigations make it possible to verify the simulation results in a different way from auroral observations (Shao et al., 2002). In ground-based observations, effects of the Pedersen current and the FAC are canceled with each other by Fukushima's theorem (Fukushima, 1976). In the global simulation hitherto, therefore, the ground magnetic variation is often reproduced assuming only the contribution from the Hall current (Fujita, Tanaka, Kikuchi, Fujimoto, Hosokawa, et al., 2003; Fujita, Tanaka, Kikuchi, Fujimoto, & Itonaga, 2003; Fujita et al., 2005; Kitamura et al., 2008). This approximation is valid only under a uniform ionosphere and magnetic field lines that are perpendicular to the ionosphere. These conditions will be met to some extent at high latitudes on the dayside.

1.3. The SC and the Substorm

Fujita, Tanaka, Kikuchi, Fujimoto, Hosokawa, et al. (2003), Fujita, Tanaka, Kikuchi, Fujimoto, and Itonaga (2003), and Fujita et al. (2005) investigated the correspondence between the SC current system and ground magnetic perturbations. In these studies, ground magnetic perturbations were estimated from simulation results under the assumption that Fukushima's theorem is satisfied. These researches reproduced the preliminary impulse (PI) and main impulse (MI) on the dayside in midlatitudes, the structure of the magnetospheric current system that generates them, and the correspondence between each current system and magnetic field variations. On the nightside in the middle and low latitudes, however, it may be difficult for the Fukushima's theorem to be satisfied since the ionospheric conductivity there is too low for the ionospheric current connected to the FAC to reach just above. It is insufficient in these regions to evaluate ground magnetic variations only from the Hall current. Also in the equatorial region, the conditions under which the Fukushima's theorem holds may be hardly realized. That is because there is a nonuniform structure called Cowling conductivity in the equatorial region. This may also be evidenced from peculiar SC variations at the equator (Sastri et al., 2001).

In the substorm, magnetic field perturbations in the auroral oval are mostly due to the Hall current. While the FAC is connected to the auroral oval where the electric conductivity is high, the ionospheric current connected to the FAC mainly flows along the auroral oval. Such ionospheric current does not leak out to middle and low latitudes in the night, because the electric conductivity is low there. Thus, midlatitude ionospheric current connected to the FAC will contribute little to the magnetic field variation and will not be effective in canceling the contribution of the FAC. At postmidnight, such insufficient canceling generates an increase in the X component. The positive bay is thought to occur by such mechanism (Reddy et al., 1988; Hashimoto et al., 2011).

The magnetic field variations can be more accurately evaluated from Biot-Savart's law with the solution of the global simulation. This evaluation enables the global verification of various models for ground magnetic field variations. In particular, we would like to examine how does Fukushima's theorem influence actual variations of ground magnetic field. In this paper, the solar wind is given so as to generate the SC and the substorm, to reproduce magnetic field fluctuations on the ground for these events. Based on these results, we will examine individual roles of four current components to ground magnetic variations, including how their roles change depending on latitude and local time, and how strictly Fukushima's theorem holds in each case. In the substorm, we particularly try to investigate the positive bay. From these results (ground magnetic variations), we would like to verify the model of conductivity set in the global simulation, and correctness of the current understanding for diffuse auroral effects on the ionospheric conductivity. Ground magnetic variations have been studied for a long time to have given many plausible current models causing them. If ground magnetic variations are reproduced as observed, we can verify current systems and effective current components. At the same time, we can verify the global simulation as the tool that gives correct numerical solutions.

2. Method of Numerical Calculation

In the present paper, the magnetosphere-ionosphere disturbances are reproduced by REPPU (REProduce Plasma Universe) code. In the solar wind and magnetospheric regions, the basic equation is the MHD equation discretized by the total variation diminishing scheme (Tanaka, 2000). In the ionosphere, the basic equation is the current continuity condition. The calculation range of the MHD equation is the 3-D domain from 3 to 300 Re, and a total of 46,695,160 grid points is allocated in this domain. An unstructured grid system that has no grid concentration point is generated so as to realize stable computation under allocation of many grids on the inner boundary. From this scheme, the number of grid points on the inner boundary is 122,882. Supporting information shows the process to generate the grid system. Outer boundary condition at downtail (300 Re) is zero gradient condition. Inner boundary conditions are given depending on the structure of characteristic lines in the hyperbolic equation. How to set these inner boundary conditions was presented in detail in Tanaka, Obara, et al. (2017).

The ionosphere is a 2-D thin spherical shell at 1.016 Re. The grid points on the inner boundary at 3 Re is projected down along the dipole field to the ionosphere at 1.016 Re. Projected points are used as ionospheric grid coordinates. Since this projection extends only as low latitude as 55°, the lower-latitude region of the

ionosphere is covered by another structured grids. The whole ionosphere is covered by grids about twice 122,882. In such a configuration, the grid spacing is about 0.3° in the ionosphere. The magnetosphere and the ionosphere forms a coupling system, by exchanging potential and the FAC along the dipole magnetic field.

The ionospheric conductivity is determined as the function of the solar zenith angle, pressure, temperature, and the FAC. Here, pressure, temperature, and the FAC are projected along the magnetic field from 3 to 1.016 Re. For the contribution of the solar zenith angle, the Pedersen conductivity in the subsolar region is set to 3.6 mho. The Hall to Pedersen ratio is 1.8 for the component depending on the solar zenith angle, and 3.5 for others. This ratio reflects the difference between ionization by the solar extreme ultraviolet and ionization by particle precipitation. The ionospheric conductivity at the magnetic equator (Cowling effect) is calculated according to Tsunomura (1999). Such setting of the ionospheric conductivity has a great influence on simulation results. For example, dependence of ionospheric conductivity on the FAC strongly controls appearance of the WTS (Ebihara & Tanaka, 2015b). Ionospheric current system must also reflect the diffuse aurora (simulated by projected pressure and temperature) and Cowling effect. In this paper, we try to verify these settings from comparison with observations.

The initial condition of the calculation is a quasi-stationary state under the northward IMF. The solar wind conditions at this time are: density 5 cm^{-3}, $Vx = -350$ km/s, temperature 350,000 K, magnetic field ($Bx = 0.0$ nT, $By = -2.0$ nT, $Bz = 4.0$ nT). This state is common for the SC and the substorm. The SC is generated by increasing the solar wind dynamic pressure. This increase is generated by changing the solar wind density to 12 cm^{-3} and velocity to −450 km/s. The substorm is generated by reversing the IMF Bz to southward. This solar wind is given by the magnetic field ($Bx = 0.0$ nT, $By = -3.6$ nT, $Bz = -3.9$ nT). Let define $T = 0$ min when the changed solar wind reaches $X = 40$ Re. Here, the X axis is directed to the sun, the Y axis is directed in the opposite direction to the Earth's revolution, and the Z axis is directed to the north. The axis of the dipole magnetic field and the earth rotation axis are all parallel to the Z axis.

Using the solution in the magnetosphere-ionosphere coupling system, Biot-Savart's law is applied to obtain each component of the ground magnetic field variations. Since the calculation range of the REPPU code is from 3 to 300 Re, the current is not calculated in the region from 1.016 to 3 Re. In this region, the current distribution is determined by extending the FAC from 3 to 1.016 Re. Assuming that only the FAC exist in this region as current systems, the FAC is extended adopting its intensity being inversely proportional to the cross section of the magnetic field. Finally, the ground magnetic variation is obtained by dividing it into four components. The contribution of ionospheric current is divided into Hall current component and Pedersen current component. Contributions of these currents are integrated not only in the ionosphere directly above, but throughout the entire spherical shell. However, the largest contribution is given from immediately above the observing point in closest proximity. Contributions of currents in the magnetosphere is divided into the component of the FAC in the region of 1.016 to 6 Re and the component of other magnetospheric currents. Other magnetospheric currents include the CF current, the cusp current, and the tail current. The sum of these four components is called the total. This separation can be applied to three components, X (northward component), Y (eastward component), and Z (vertical component) of the magnetic field respectively. In this paper, variations of the X component are shown in the following part.

3. Reproduction of the SC

In the global simulation, the PI current system and the MI current system are reproduced as SC current systems (Fujita, Tanaka, Kikuchi, Fujimoto, Hosokawa, et al., 2003; Fujita, Tanaka, Kikuchi, Fujimoto, & Itonaga, 2003; Fujita et al., 2005). The PI lasts about 2 min from the start of the SC. The MI is a subsequent period of about 8 min. It has already been shown that the PI current system is formed by connecting the CF current under the increased magnetopause current on the dayside, the current on the surface of the compression region in the magnetosphere, the FAC, and the ionospheric current. The three-dimensional configuration of this current system has also been given by Fujita, Tanaka, Kikuchi, Fujimoto, Hosokawa, et al. (2003). Similarly, Fujita, Tanaka, Kikuchi, Fujimoto, and Itonaga (2003) showed that the subsequent MI current occurs in association with convection transient. This transient convection is driven as the process to realize a new steady convection that matches with the changed boundary conditions. The FAC in this process is generated similarly to the Region 1 FAC in the ordinary case. The dynamo for the MI current is in the cusp-mantle

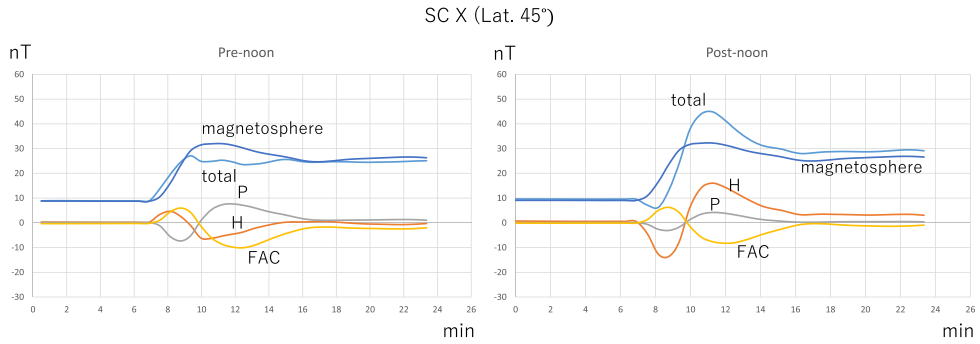

Figure 1. Magnetic components that construct the SC (*X* component) on the dayside at 45° latitude. The left panel shows the prenoon case, and the right panel shows the postnoon case. Suffixes H, P, FAC, and magnetosphere show contributions of the Hall current, the Pedersen current, the FAC, and other magnetospheric currents to the variation of ground magnetic *X* component. Total shows the sum of four components.

region (Tanaka et al., 2016). This dynamo converts thermal energy into electromagnetic energy. The plasma motion that drives this dynamo is the slow mode expansion (Watanabe et al., 2019).

3.1. Dayside SC

Figure 1 shows the dayside SC (*X* component) in midlatitude (45°) and variations of four components that constitute the SC. Total is the sum of four components. The left panel is result for the pre-noon region and the right panel is result for the post-noon region. In the transient stage within 10 min from the SC onset, all of variations due to the Hall current, the Pedersen current, the FAC, and the magnetospheric current give considerable contributions to the total, in both panels. Among these currents, it is the magnetosphere current that causes the main part (stepwise increase of the *X* component) of the SC variation. The main part of this variation in magnetospheric current is given by the increase in the CF current. This part can explain the classical SC picture. After 10 min, the magnetospheric current becomes the only contributing component for the total, and the other components tend to disappear.

Variations of four components appear to develop in two stages, the first 2 min corresponding to the PI and the next 8 min corresponding to the MI. The time of 2 min is recognized from variations of the Hall current, the Pedersen current, and the FAC. Their polarities reverse from the PI part to the MI part. However, 2 min interval will not be recognized from observations, since in the observation only the total is known and component-to-component variations are not visible. In the actually observed total component, the PI variation is differently characterized in the morning and in the afternoon. In the afternoon, it is characterized by an appearance of the PRI. Looking at the PRI in the afternoon from the total component, the duration of the PRI is 1 min. The period of the PI is 2 min in terms of variations in each component, but it cannot be identified that it is actually 2 min. From observations, the PI period will be recognized in half, that is, a minute, because observation detects only total that has negative period for one minute. It can be seen that this one minute is the result of competition between the magnetospheric current component and the Hall current component. On the morning side, identifying of 2 min is even more difficult. In the PI period, the effect of the magnetosphere current and the effect of the Hall current overlap in the positive sign, and it is difficult to specify the PI itself. Thus, it can be concluded that it is the Hall current that causes the morning-evening asymmetry of the dayside midlatitude SC.

According to Figure 1, the Pedersen current effect and the FAC effect are almost canceled out both in the PI and the MI intervals. That is, Fukushima's theorem holds to some extent, although not perfect. The FAC effect seems to be dominant over the Pedersen current effect, though only slightly. Still, the magnetic field variations are approximately the sum of the magnetospheric current effect and the Hall current effect. According to Fukushima's theorem, the effects of the Pedersen current and the FAC cancel each other, so it is the Hall current effect that apparently generates the PRI on the afternoon side. On the morning side, the polarity of Hall current effect is reversed, and the Hall current effect can no longer be the PRI. Since the effects of the FAC and the Pedersen current cancel out, the remaining Hall current effect on the morning side can generate only the PPI. However, in Figure 1, it will be masked by the effect of the magnetospheric current changing in the same polarity to the effect of the Hall current, and it will not be clearly recognized as

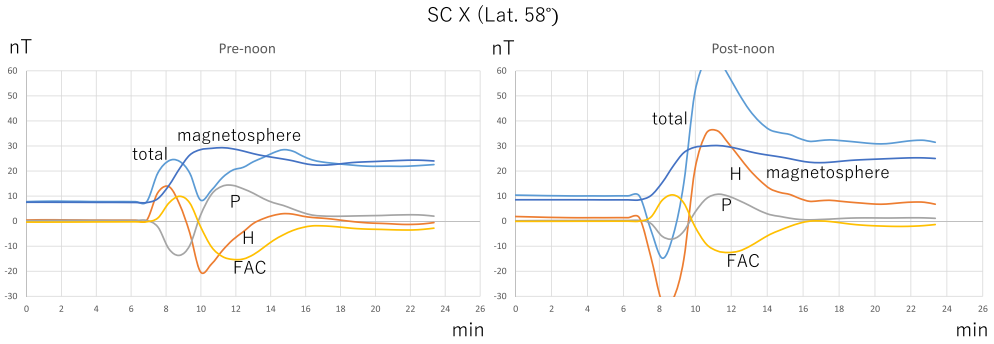

Figure 2. Magnetic components that make up the SC (*X* component) on the dayside at 58° latitude. The left panel shows the prenoon case, and the right panel shows the postnoon case. Suffixes H, P, FAC, and magnetosphere shows contributions of the Hall current, the Pedersen current, the FAC, and other magnetospheric currents to the variation of ground magnetic *X* component. Total shows the sum of four components.

the PPI. For the Hall current, the Pedersen current and the FAC in the MI period, the timings of the strongest influence appear with time differences, and their superposition gives a wavy fluctuation to the total.

Figure 2 shows the day side SC (*X* component) at a higher latitude (58°). A comparison of Figures 1 and 2 reveals the latitude effect in the daytime. At high latitudes, Fukushima's theorem seems to be more rigorous. The amplitude of the Hall current effect increases at high latitudes, and its effect appears to be larger. This is because the observing point approaches the source region. The amplitude of the Pedersen current effect also increases but cancels with the FAC effect, and the effect of the increase apparently does not appear in the total. As a result, the PRI becomes larger in amplitude on the afternoon side, since the ratio of the Hall current to the total becomes stronger. Also, the MI will become larger and clearer on the evening side. On the morning side, on the contrary, the PPI can be seen by the effect of the Hall current. Compared to the results in 45° latitude, the PPI becomes more visible in the total, because the effect of the Hall current increases while the magnetospheric current does not change so much. Due to the increased influence of the Hall current, the MI becomes less clear in the morning, and its peak appears to be much later, even if it exists.

3.2. Nightside SC

Figure 3 shows the SC variation (*X* component) at night. The left panel is for the premidnight and the right panel is for the postmidnight. At night, the contribution of ionospheric currents for the total is generally small because the ionospheric conductivity is low. For this reason, Fukushima's theorem does not hold. That is, the FAC effect is not canceled out by the Pedersen current effect. Therefore, the total is approximately the superposition of the magnetospheric current effect and the FAC effect. The variation of the *X* component due to the FAC effect itself is a bit smaller than that on the dayside. This is because the nightside is somewhat farther from the low-altitude part of the FAC. A main contribution to the FAC effect is given by

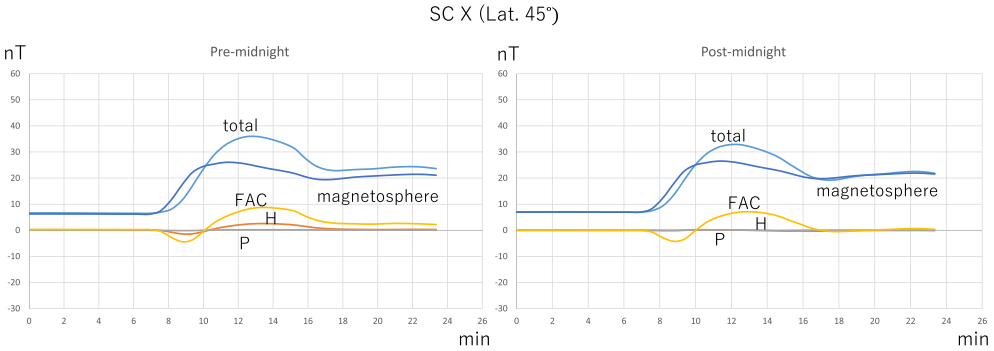

Figure 3. Magnetic components that construct the SC on the nightside at 45° latitude. The left panel shows the premidnight case, and the right panel shows the postmidnight case. Suffixes H, P, FAC, and magnetosphere shows contributions of the Hall current, the Pedersen current, the FAC, and other magnetospheric currents to the variation of ground magnetic *X* component. Total shows the sum of four components.

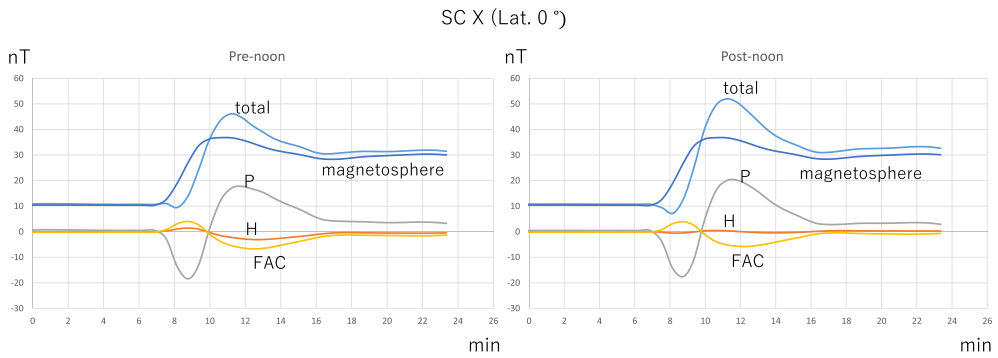

Figure 4. Magnetic components that construct the SC (*X* component) at the dayside equator. The left panel shows the pre-noon case, and the right panel shows the postnoon case. Suffixes H, P, FAC, and magnetosphere shows contributions of the Hall current, the Pedersen current, the FAC, and other magnetospheric currents to the variation of ground magnetic *X* component. Total shows the sum of four components.

the FAC part close to the Earth. In the PI current system shown by Fujita, Tanaka, Kikuchi, Fujimoto, Hosokawa, et al. (2003), the FAC during the PI distributes on the dayside, so that the nightside region is somewhat far from the FAC.

In Figure 3, the polarity of the FAC effect is opposite to daytime in Figures 1 and 2. The effect of the FAC gives negative *X* variations in the PI part and positive *X* variations in the MI part. These polarities are the same both before and after midnight, and the asymmetry of morning and evening is small on the night side. This aspect is clearly seen in Figure 3. The polarity of the FAC in Figure 3 shows a possibility to generate the PRI at night. In Figure 3, however, the FAC effect is not large enough to cause the nighttime PRI. Even in the real observation, no result has ever reported for the night PRI in midlatitude.

3.3. SC in the Equatorial Region

Figure 4 shows the SC variations (*X* component) at the dayside equator. It can be seen from Figure 4 that dominant contributions to the SC at the equator come from effects of the magnetospheric current and the Pedersen current. The dominance of the Pedersen current is due to the Cowling conductivity. At the equator, the Pedersen current effect does not cancel out with the FAC effect. First of all, the equator is far from the FAC. In addition, the Cowling component is dominant for ionospheric conductivities. These situations deviate from the condition under which Fukushima's theorem holds. If the conductivity of observing point is much higher than that of the FAC connection point, then Fukushima's theorem no longer holds.

In Figure 4, the PRI occurs both in the morning and in the afternoon, but this variation is due to the Pedersen current. The midlatitude PRI is due to the effect of the Hall current, so its polarity limits the PRI to the afternoon. At the equator, however, the Pedersen current has the polarity to generate the PRI both in the morning and in the afternoon. In Figure 4, the PRI is a little affected by the Hall current although its effect is weak. The polarity of the Hall current effect is reversed in the morning and the afternoon. In the morning, the polarity of the Hall current effect is to weaken the PRI. On the other hand, on the afternoon side, the Hall current has a polarity to strengthen the PRI. However, the influence of these Hall currents is extremely weak, and the influence of the Pedersen current prevails both in the morning and in the afternoon as the PRI. These features in the equator will also depend on the method of modeling the Cowling conductivity (Tsunomura, 1999).

It is found from Figure 4 that the PRI at the equator is generated by the Pedersen current. This is in contrast to the midlatitude PRI due to the Hall current effect. In order to see the local time (LT) dependence of the PRI in the equator, Figure 5 shows variations of the total component at various LTs. It can be seen from Figure 5 that the PRI is generated at 10–14 LT. From the observation, it is also concluded that the PRI at the magnetic equator occurs around midday (Sastri et al., 2001). In Figure 5, the amplitude of the MI following the PRI is 25 nT at midnight and 45 nT at midday. Comparing with Figure 4, it can be estimated that the midnight MI is almost only the contribution of the magnetospheric current. Thus, the contribution of the Pedersen current to the MI is up to 20 nT on the dayside. When the PRI is pronounced, the contribution of Pedersen current to the MI also becomes large.

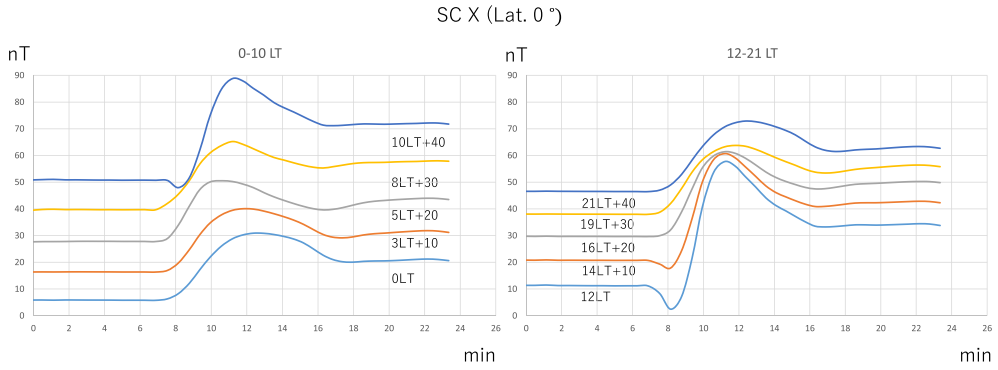

Figure 5. LT dependence of the equatorial H variations during the SC. The left panel shows 0–10 LT, and the right panel shows 12–21 LT. The equatorial PRI occurs around the noon.

It can be seen from Figure 4 for the equatorial region that effects of the FAC and the Hall current are relatively weak compared with the effect of the Pedersen current. The equator is far from the FAC, and the influence of the FAC becomes weak. From the result of calculation in Figure 5, no PPI is recognized in any LT. In the observation, however, the PPI is occasionally observed at the nighttime equator (Araki et al., 1985). Since the polarity of the Pedersen current is reversed at night, the PPI may be possible if the ionospheric conductivity stays high at night.

4. Substorm Disturbances

The primary factor that makes us recognize the substorm may be auroral observations. The main auroral events during the substorm will be the quiet arc during the growth phase, the initial brightening at the onset, and the WTS during the expansion phase. Recent global simulations have reproduced the occurrences of these auroras as a series of events (Tanaka, 2015; Ebihara & Tanaka, 2015a, 2015b, 2016; Tanaka et al., 2010, Tanaka, Ebihara, et al., 2017; Tanaka, Ebihara, et al., 2019). Another phenomenon that characterize the substorm, as well as the aurora, may be the global variation of geomagnetic field. Both the aurora and the magnetic field variation are phenomena connected to the FAC and convection (Tanaka et al., 2016).

The fundamental role of convection is to form a pathway to transport, dissipate, and discharge stress caused by the solar wind-magnetosphere interaction (Tanaka, Obara, et al., 2019). Stress is first converted to thermal energy through force balance. Main part of thermal energy is released through the mantle or the low-latitude boundary layer. A part of thermal energy is allocated to generate the FAC by converting thermal energy to electromagnetic energy (Tanaka et al., 2016). This FAC acts to release energy to the ionosphere (Ebihara & Tanaka, 2017; Ebihara et al., 2019). The FAC at the same time acts to transfer convection to the ionosphere. An important problem is how the dynamo that drives the FAC performs energy conversion. In the concept of convection driven by the tension of the open magnetic field, the dynamo is excited by deceleration of magnetosheath flow (Wilder et al., 2015). However, this mechanism is not realized by the simulation.

The FAC and magnetic field variations during the substorm reflect the process by which convection under the southward IMF is transmitted to the ionosphere as the two cell convection. Associated with the onset, path of return convection in the tail is changed from the lobe-plasma sheet boundary to the plasma sheet center (Tanaka, Ebihara, et al., 2017). This change occurs in synchronous with the transition of the tail topology (Tanaka, Ebihara, et al., 2019). These processes are often understood by a simplified picture that the NENL is formed to release flow jet from it. Under such simplification, the onset current is understood by the CW. To be precise, however, the dynamo is essential for the FAC generation (Watanabe et al., 2019). This situation is realized at the onset by the near-Earth dynamo that generates the onset FAC (Ebihara & Tanaka, 2015a). Here in this paper, we try to reproduce ground magnetic variations associate with the onset and its causing current system. In this process, the upward FAC is recognized as arc auroras, and the FAC and the ionospheric current linked to it give ground magnetic field variations.

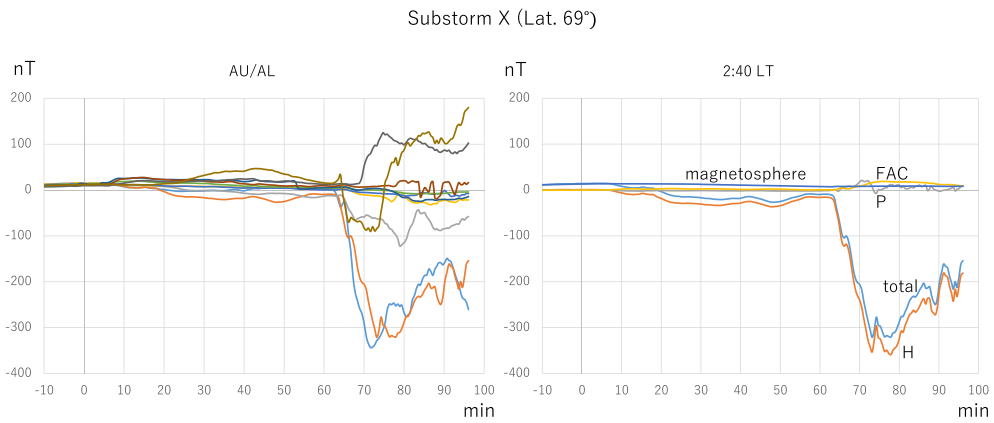

Figure 6. AU/AL indices reproduced by the global simulation (left) and the decomposition of the postmidnight variation (2:40 LT) to four components (right). The growth phase, the onset, and the expansion phase are identified from the AU/AL indices. Suffixes H, P, FAC, and magnetosphere shows contributions of the Hall current, the Pedersen current, the FAC and other magnetospheric currents.

4.1. Magnetic Variations in the Auroral Region

For the ground magnetic field observation during the substorm, the most characteristic magnetic field variation is given by the auroral electro jet (AEJ). The global aspect of this magnetic field variation can be seen from the AU/AL indices. As is well known, the AU/AL indices are upper and lower envelopes of the *X* component variations along the auroral oval. It is commonly considered that the Hall current gives a main contribution to the AU/AL indices. The left panel of Figure 6 shows the AU/AL indices (*X* stacking plot) reproduced from the substorm simulation. In such substorm simulation, the reproduction of AU/AL indices is first of all the necessary condition for the verification of the numerical solution. As shown in Figure 6, the credibility of the solution is confirmed from the reproduction of sustained fluctuations of the AU/AL indices about 50 nT in the growth phase and a sharp decrease in the AL index associated with the onset. Various substorm studies based on the numerical solution become more reliable if the realistic reproduction of ground magnetic observations is obtained.

The right panel of Figure 6 shows the variations of four components in the postmidnight area, when the most remarkable contribution is given to the decrease of the AL during the expansion phase. It turns out from this figure that it is mostly the Hall current that gives the AL index. Prevailing of the Hall current continues even from the growth phase. The contributions of the Pedersen current and the FAC are small from the first. Therefore, whether they cancel for each other or not has little meaning on evaluation of the total. For substorm magnetic variations in the polar region, therefore, with or without Fukushima's theorem does not affect the result so much. This result for the AU/AL indices contradicts with the fact that Fukushima's theorem is effective to understand the midlatitude SC. This is because the FAC associated with the SC is connected to the dayside region where the ionospheric conductivity is relatively uniform (Fujita, Tanaka, Kikuchi, Fujimoto, Hosokawa, et al., 2003, Fujita, Tanaka, Kikuchi, Fujimoto, & Itonaga, 2003).

The following points may be considered as the explanation for results obtained hitherto in the AU/AL. First, the Hall to Pedersen ratio of the ionospheric conductivity is set to 1.8 for the solar extreme ultraviolet ionization, while it is set to 3.6 for the particle precipitation effect in the polar region. This makes the effect of the Hall current relatively large in the polar region. This value 3.6 has a significant impact on the aurora dynamics during the substorm. If this value is smaller, the WTS will not be reproduced (Ebihara & Tanaka, 2015b). Next, there is the nonuniformity for the conductivity along the auroral oval. This allows the FAC to close with the Hall current (Tanaka, 2001). Thus, the Pedersen current becomes relatively weak to make Fukushima's theorem not hold. In the right panel of Figure 6, the effect of the Pedersen current does not increase even after the onset. The effect of current concentration due to nonuniform ionospheric conductivity is also important. If the current is concentrated in a narrow channel, it will lead to a large magnetic field variation just below the channel. This is identified as the Cowling effect, in which the Hall current generated by the polarization field gives a large magnetic variation.

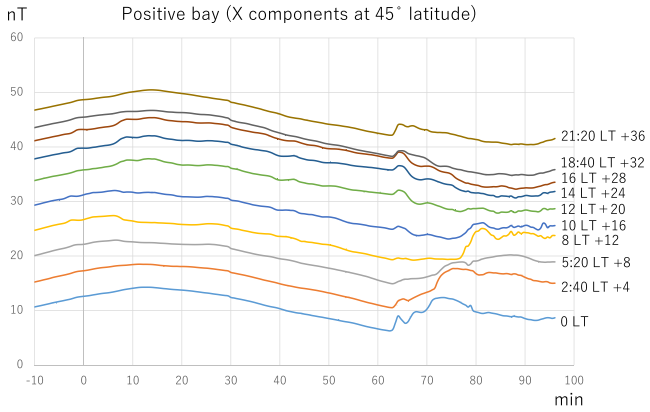

Figure 7. Time variations of the *X* component at 45° latitude at 10 points fixed to the local times. The positive bay is observable in the postmidnight.

4.2. Positive Bay

At high latitudes, the variation of the AU/AL indices during the substorm is mostly generated by the effect of the Hall current. Then how is the midlatitude? Figure 7 shows variations of the *X* component at midlatitude (45°) for the same substorm illustrated in Figure 6. In Figure 7, the variations of the *X* component at midlatitude exhibit a dependency on the LT. In the postmidnight region, the *X* component begins to increase along with the substorm onset. The start of the increase is simultaneous with the onset, but the time to reach the peak is earlier near the midnight and becomes later as it goes to the dayside. Also, such variations are noticeable at postmidnight, but are not clearly visible at pre-midnight. It is not visible even on the dayside.

Figure 8 shows the contribution of each of the four components to the magnetic field variation corresponding to the positive bay in the middle latitude (45°) in the postmidnight. Similar to the case of the SC, four components and the total are displayed as components of magnetic field variations. In Figure 8 (left), the FAC effect is calculated by considering the FAC from 1 to 6 Re. On the other hand, Figure 8 (right) shows the same display as the left but shows the result when the FAC is restricted to only the portions from 1 to 3 Re. During the growth phase, the magnetospheric current component mainly contributes to the total, with a small contribution of the FAC. Such variation indicates that the global magnetic field structure and the current system accompanying it are changing significantly along with the development of convection in the growth phase. It can be seen for the period of the growth phase that Fukushima's theorem hardly holds at midlatitude at night.

As can be seen in Figure 8, it is mainly the effect of the FAC that causes the variation of the positive bay. In addition, an appreciable effect is given by the magnetospheric current. Even when the effect of the FAC is

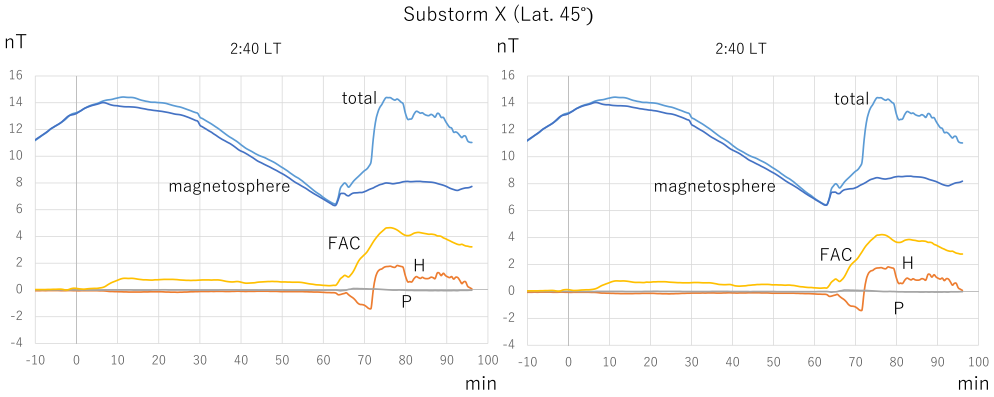

Figure 8. The positive bay (*X* component) in the postmidnight at 45° latitude. The left panel shows the case in which contribution of the FAC is considered from 1–6 Re, and the right panel shows the case in which contribution of the FAC is considered from 1–3 Re. Suffixes H, P, FAC, and magnetosphere shows contributions of the Hall current, the Pedersen current, the FAC, and other magnetospheric currents to the variation of ground magnetic *X* component.

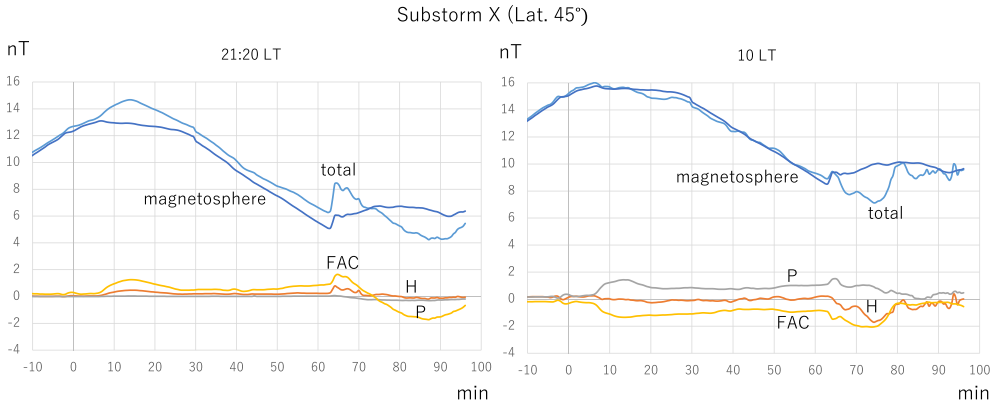

Figure 9. Time variations of the *X* component at 45° latitude in the premidnight (left) and on the dayside (right). The left panel shows the premidnight case, and the right panel shows the dayside case. Suffixes H, P, FAC, and magnetosphere shows contributions of the Hall current, the Pedersen, the FAC, and other magnetospheric currents to the variation of ground magnetic *X* component.

limited to 1 to 3 Re as shown in Figure 8 (right), the result changes only little. In other words, the contribution of the FAC as a cause of positive bay mostly comes from the FAC part close to the earth. Somewhat irregular structure of the positive bay caused by the Hall current effect is not seen in observations. This result suggests that the nightside ionospheric conductivity may be still larger than the real value.

In the middle latitude at night, Fukushima's theorem does not hold both in the growth phase and the expansion phase. The positive bay is a break of Fukushima's theorem itself. The FAC connects to the high-latitude ionosphere, but the related ionospheric current does not reach to low latitudes at night. Therefore, Fukushima's theorem does not hold in this case, and only the effect of FAC becomes remarkable at low latitudes. Also, the Hall current is weak and does not give a significant effect to the total. These are the reason why the cause of positive bay is the FAC. If there are a downward FAC in the morning and an upward FAC in the evening, an increase in the northward magnetic field due to this FAC is expected near midnight. If Fukushima's theorem does not hold, only the FAC effect is visible on the ground and it will be observed as the positive bay.

If the FAC effect is symmetric with respect to the morning and the evening, then the positive bay will also be symmetric in the morning and the evening. Figure 9 shows results at another LTs (premidnight and dayside). In the comparison between Figures 8 (left) and 9 (left), difference is apparent in the influence of the FAC. This effect is the reason why the morning and evening symmetry is broken in the positive bay. It can be seen in Figure 9 (right) that the FAC effect cancels with the Pedersen current effect on the dayside. Some influence of the Hall current remains for the variation of the total after the onset. That is, on the midlatitude in the dayside, Fukushima's theorem holds to some extent even in the substorm.

4.3. Development of the FAC

Consequently, it can be understood from Figures 7–9 that the positive bay is the case where the effect of the FAC is directly visible at midlatitudes in the night. As shown in Figure 7, however, the positive bay has an asymmetry between the premidnight and the postmidnight. We further analyze the cause of this asymmetry. Figure 10 shows how the LT distribution of the FAC changes before and after the onset. Here, the FAC is the sum along the latitude, and is the net FAC at a certain longitude. Thus, it is the sum of both the Region 1 FAC and the Region 2 FAC. Before the onset, the net FAC is still weak along all longitudes. At the onset, both the Region 1 FAC and the Region 2 FAC increase, but the sum is upward (−) on the evening side and downward (+) on the morning side. That is, the net FAC is in the sense of the Region 1 FAC. The peak of the Region 1 FAC (upward) in the evening exists stably near the midnight without remarkable movement. On the other hand, the peak position of the morning Region 1 FAC (downward) tends to move from the midnight toward the dawn with time after the onset. This variation can explain the LT dependence of the positive bay in Figure 7.

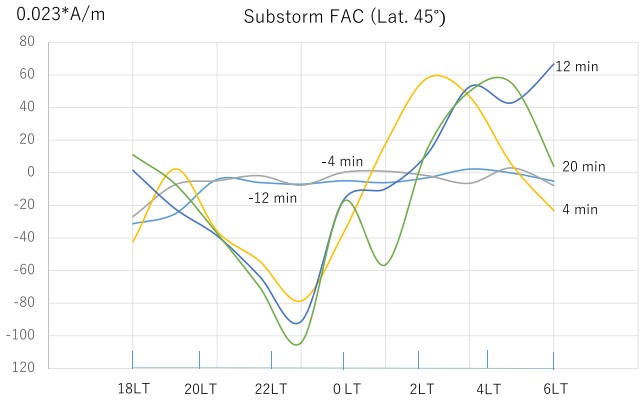

Figure 10. Local time distributions of the net FAC before and after the substorm onset. Time notations in this figure are the passage time from $T = 62.5$ min (onset time).

The asymmetry of the positive bay is caused by the asymmetrical distribution of the FAC in longitude. So what causes this FAC asymmetry? In the Region 1 FAC area in ionosphere, the ionospheric conductivity is first influenced by pressure and temperature throughout the auroral oval. Before midnight, ionospheric conductivity is in addition accompanied by an increase due to the upward FAC. Therefore, the conductivity is large on the evening side. This is expected to act as the cause of the asymmetry of the Region 1 FAC. To see this situation, Figure 11 shows distributions of the FAC and electrical conductivity 20 minutes after the onset. The evening Region 1 FAC is concentrated near the midnight around 22:30 LT. This is consistent with the results of Figure 10. Electrical conductivity is increased in the area where FACs are concentrated. This is because electrical conductivity is increased by the Region 1 FAC itself. On the other hand, in the morning Region 1 area, there is no local increase in electrical conductivity, but a uniform LT distribution is realized. Therefore, the Region 1 FAC is flatly distributed over the postmidnight region. A similar FAC structure to Figure 11 is obtained also from satellite observations (Clausen et al., 2012). However, the observation shows a large asymmetry between the northern and southern hemispheres. On the other hand, the simulation does not show the north-south asymmetry. The reason is unknown.

It is expected from the reproducibility of the substorm including the positive bay that the setting of the ionospheric conductivity in REPPU code is fairly adequate. The reproduction of the WTS on the evening side is indispensable for the substorm to be reproduced realistically and correctly. This process requires the increase of ionospheric conductivity by the upward FAC (Ebihara & Tanaka, 2016). This setting corresponds to the discrete aurora. In the Region 1 FAC area on the dawn side, the electric conductivity increases mainly by pressure and temperature. This setting corresponds to the diffuse aurora. The feature of the positive bay development in Figure 7 indicates that these settings in REPPU code are reasonable. Although it is difficult

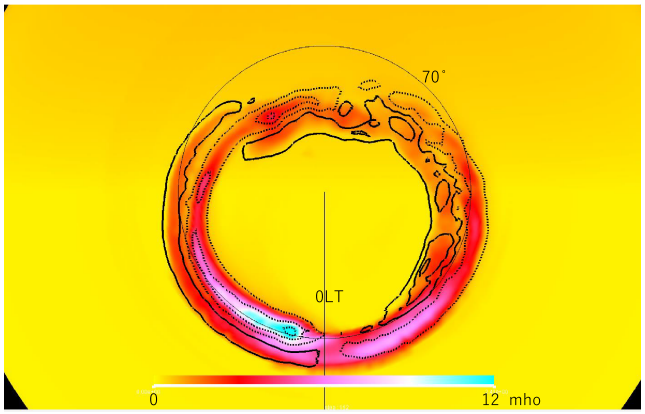

Figure 11. Distributions of the FAC (contours) and the Hall conductivity (color shadings) in the ionosphere 20 min after the onset. Solid contours show the downward FAC, and dashed contours show the upward FAC. Contour interval is 0.4 $\mu A/m^2$.

to verify the conductivity setting in the global simulation, reproductions of the positive bay as well as the WTS give some reliability for this problem.

5. Discussion and conclusion

In this paper, we investigated current systems which give the ground magnetic field variations in the SC and the substorm. Currents considered here are the Hall current of the ionosphere, the Pedersen current of the ionosphere, the FAC, and the magnetospheric current other than the FAC. From the solution of the global simulation and Biot-Savart's law, we investigated on which of the four components the magnetic field variation on the ground at certain point and certain timing depends. These investigations show that the models of ground magnetic variations estimated hitherto based on observations are, for the most part, correct. As a result, this paper has not found a new mechanism for ground magnetic field variations, but has confirmed that many of causative currents estimated so far are adequate both qualitatively and quantitatively. Through these results, the global simulation model is also verified from the comparison with ground magnetic field variations. It is quite significant to conclude that the global simulation gives not only correct solutions for the magnetospheric structure but also correct connectivity between the ionosphere and the magnetosphere.

The main part of the SC is generated by the magnetospheric current. As expected commonly, this is the effect of the CF current. Among SC variations, the midlatitude PRI occurs due to the effect of the Hall current. In this case, the polarity of the Hall current alternates in the morning and the afternoon, and the PRI occurs only in the afternoon where the Hall current gives a negative fluctuation. The influence of the Hall current may be the PPI in the morning, but it is difficult to see the PPI because the Hall current effect has the same polarity as the magnetospheric current. However, as the observing point approaches high latitudes, it will become clearly visible. Thus, the pattern where the PPI occurs in the morning and the PRI occurs in the afternoon is the case in which Fukushima's theorem is satisfied, where only the Hall current effect becomes visible.

Mechanisms that determine the ionospheric current are more local than that of the FAC. Ionosphere current may decrease locally depending on the season and the location. Under such condition, the midlatitude PPI can be generated by the FAC effect as well as the Hall current effect in the morning (Kikuchi et al., 2001). The polarity of the FAC in Figure 1 is indeed so. If the ionospheric conductivity decreases significantly, effects of the Hall current and the Pedersen current become relatively small, and there is a possibility to generate the PPI by the FAC effect. For example, winter may meet such conditions (Kikuchi et al., 2001). In this case, Fukushima's theorem is broken. However, such PPI does not occur under the conditions set in this paper.

The equatorial PRI (Kikuchi et al., 2001) is the effect of the Pedersen current. The polarity of the Pedersen current effect is the same in the morning and the afternoon. Therefore, the equator PRI can occur both in the morning and in the afternoon. In observations, the equatorial PRI occurs mainly around noon (Kikuchi et al., 2001) and occurs even in the morning (Sastri et al., 2001). These observations are consistent with the prediction of the global simulation. The predominance of the Pedersen current effect at the equator is due to the Cowling effect, where Fukushima's theorem does not hold.

Seen from their disturbance levels, the SC and the substorm are phenomena that are very different from each other. The variations of the AU/AL indices of the substorm is 10 times larger than that of the SC. However, as disturbances seen from currents in the magnetosphere, the SC and the substorm are not so different in magnitude. By comparing Figures 1 and 2 with the right panel of Figure 6, it can be seen that there is no difference in the magnitude of the FAC effect. The difference between the two events would be the difference in the magnetosphere-ionosphere coupling. These causes may be the synthesis of several effects. In the polar region, the increase in conductivity due to aurora is large through the upward FAC. In addition, the large Hall-Pedersen ratio makes the Hall current stronger. Since the Hall current flows in a narrow channel, magnetic field variations become larger immediately below the channel due to the concentration of current. The narrow channel causes polarization in the ionosphere and further strengthens the Hall current. As a result, conditions for Fukushima's theorem are hardly satisfied under the process where the AEJ associated with the substorm gives strong variations of ground magnetic field.

Due to the effect of Fukushima's theorem, the Hall current is generally considered to contribute most to ground magnetic field variations. This is true for a substantial part of the SC, but not in every cases. The equatorial PRI is an example for the break of Fukushima's theorem, where the Pedersen current gives a major contribution due to the break of Fukushima's theorem. In addition, the positive bay during the substorm is an example of Fukushima's theorem break and a major contribution is given from the FAC. Thus, ground magnetic field variations that have been traditionally recognized as extraordinary variations very often correspond to cases where Fukushima's theorem is broken.

Although the original application target of Fukushima's theorem may be the substorm AEJ, Fukushima's theorem hardly holds there due to the strong nonuniformity of the electric conductivity. For the AEJ, conditions for Fukushima's theorem is not effective from the beginning. Due to the channel structure of the AEJ, the effect of the Hall current is magnified to a large extent, while effects of the Pedersen current and the FAC do not become large.

Generally, global simulation models include two major uncertainties. They are the settings of magnetic diffusion and the ionospheric conductivity. Magnetic diffusion has been verified to some extent through the reproduction of the substorm expansion (Tanaka et al., 2010). Also, the ionospheric conductivity due to the arc aurora has been confirmed by the WTS. In this paper, it is additionally confirmed from the verification of the positive bay that the ionospheric conductivity model is set with considerable validity. In particular, the result of this paper will be a valuable verification for the setting of the ionospheric conductivity corresponding to the diffuse aurora on the dawn side, while it has not been sufficiently verified hitherto.

Acknowledgments
In the present study, we used the high-speed computing system at Polar Data Center of National Institute of Polar Research through General Collaboration Project 29-5, and the KDK computer system at the Research Institute for Sustainable Humanosphere (RISH), Kyoto University through General Collaboration Project 2019KDK-04. This study was supported by KAKENHI (Grant 15H03732) and MEXT/JSPS KAKENHI Grant 15H05815. Numerical data (coordinate data and variable data), information for graphic program, and history data necessary to reproduce drawings are available online (http://polaris.nipr.ac.jp/~reppu/reppu2/reppu6/).

References

Araki, T., Allen, J. H., & Araki, Y. (1985). Extension of a polar ionospheric current to the nightside equator. *Planetary and Space Science*, *33*, 11–16.

Clausen, L. B. N., Baker, J. B. H., Ruohoniemi, J. M., Milan, S. E., & Anderson, B. J. (2012). Dynamics of the region 1 Birkeland current oval derived from the Active Magnetosphere and Planetary Electrodynamics Response Experiment (AMPERE). *Journal of Geophysical Research*, *117*, A06233. https://doi.org/10.1029/2012JA017666

Ebihara, Y., & Tanaka, T. (2015a). Substorm simulation: Insight into the mechanisms of initial brightening. *Journal of Geophysical Research: Space Physics*, *120*, 7270–7288. https://doi.org/10.1002/2015JA021516

Ebihara, Y., & Tanaka, T. (2015b). Substorm simulation: Formation of westward traveling surge. *Journal of Geophysical Research: Space Physics*, *120*, 10,466–10,484. https://doi.org/10.1002/2015JA021697

Ebihara, Y., & Tanaka, T. (2016). Substorm simulation: Quiet and N-S arcs preceding auroral breakup. *Journal of Geophysical Research: Space Physics*, *121*, 1201–1218. https://doi.org/10.1002/2015JA021831

Ebihara, Y., & Tanaka, T. (2017). Energy flow exciting field-aligned current at substorm expansion onset. *Journal of Geophysical Research: Space Physics*, *122*, 12,288–12,309. https://doi.org/10.1002/2017JA024294

Ebihara, Y., Tanaka, T., & Kamiyoshikawa, N. (2019). New diagnosis for energy flow from solar wind to ionosphere during substorm: Global MHD simulation. *Journal of Geophysical Research: Space Physics*, *124*, 360–378. https://doi.org/10.1029/2018JA026177

Fujita, S., Tanaka, T., Kikuchi, T., Fujimoto, K., Hosokawa, K., & Itonaga, M. (2003). A numerical simulation of the geomagnetic sudden commencement: 1. Generation of the field-aligned current associated with the preliminary impulse. *Journal of Geophysical Research*, *108*(A12), 1416. https://doi.org/10.1029/2002JA009407

Fujita, S., Tanaka, T., Kikuchi, T., Fujimoto, K., & Itonaga, M. (2003). A numerical simulation of the geomagnetic sudden commencement: 2. Plasma processes in the main impulse. *Journal of Geophysical Research*, *108*(A12), 1417. https://doi.org/10.1029/2002JA009763

Fujita, S., Tanaka, T., & Motoba, T. (2005). A numerical simulation of the geomagnetic sudden commencement: 3. A SC in the magnetosphere-ionosphere compound system. *Journal of Geophysical Research*, *110*, A11203. https://doi.org/10.1029/2005JA011055

Fukushima, N. (1976). Generalized theorem for no ground magnetic effect of vertical currents connected with Pedersen currents in the uniform conductivity ionosphere. *Report of Ionosphere and Space Research in Japan*, *30*, 35–40.

Hashimoto, K. K., Kikuchi, T., Watari, S., & Abdu, M. A. (2011). Polar-equatorial ionospheric currents driven by the region 2 field-aligned currents at the onset of substorms. *Journal of Geophysical Research*, *116*, A09217. https://doi.org/10.1029/2011JA016442

Kikuchi, T., Tsunomura, S., Hashimoto, K., & Nozaki, K. (2001). Field aligned current effects on midlatitude geomagnetic sudden commencements. *Journal of Geophysical Research*, *106*, 15,555–15,565.

Kitamura, K., Shimazu, H., Fujita, S., Kunitake, M., Shinagawa, H., & Tanaka, T. (2008). Properties of AE indices derived from real-time global simulation and their implications for solar wind-magnetosphere coupling. *Journal of Geophysical Research*, *113*, A03S10. https://doi.org/10.1029/2007JA012514

Reddy, C. A., Ajith Kumar, S., & Somayajulu, V. V. (1988). An observational test for the ionospheric or magnetospheric origin of night-time geomagnetic positive bays at low and middle latitudes. *Planetary and Space Science*, *36*, 1149–1156.

Sastri, J. H., Takeuchi, T., Araki, T., Yumoto, K., Tsunomura, S., Tachihara, H., et al. (2001). Preliminary impulse of the geomagnetic storm sudden commencement of November 18, 1993. *Journal of Geophysical Research*, *106*, 3905.

Shao, X., Guzdar, P. N., Milikh, G. M., Papadopoulos, K., Goodrich, C. C., Sharma, A., et al. (2002). Comparing ground magnetic field perturbations from global MHD simulations with magnetometer data for the 10 January 1997 magnetic storm event. *Journal of Geophysical Research*, *107*(A8), 1177. https://doi.org/10.1029/2000JA000445

Tanaka, T. (2000). The state transition model of the substorm onset. *Journal of Geophysical Research*, *105*, 21,081–21,096. https://doi.org/10.1029/2000JA900061

Tanaka, T. (2001). IMF By and auroral conductance effects on high-latitude ionospheric convection patterns. *Journal of Geophysical Research*, *105*, 21,081.

Tanaka, T. (2015). Substorm auroral dynamics reproduced by the advanced global M-I coupling simulation. In Y. Zhang (Ed.), *Auroral Dynamics and Space Weather*, *Geophys. Monogr. Ser.* (Vol. 215, pp. 177–190). Washington, DC: American Geophysical Union.

Tanaka, T., Ebihara, Y., Watanabe, M., Den, M., Fujita, S., Kikuchi, T., et al. (2017). Global simulation study for the time sequence of events leading to the substorm onset. *Journal of Geophysical Research: Space Physics*, *122*, 6210–6239. https://doi.org/10.1002/2017JA024102

Tanaka, T., Ebihara, Y., Watanabe, M., Den, M., Fujita, S., Kikuchi, T., et al. (2019). Development of magnetic topology during the growth phase of the substorm inducing the onset of the near earth neutral line. *Journal of Geophysical Research: Space Physics*, *124*, 5158–5183. https://doi.org/10.1029/2018JA026386

Tanaka, T., Nakamizo, A., Yoshikawa, A., Fujita, S., Shinagawa, H., Shimazu, H., et al. (2010). Substorm convection and current system deduced from the global simulation. *Journal of Geophysical Research*, *115*, A05220. https://doi.org/10.1029/2009JA014676

Tanaka, T., Obara, T., & Kunitake, M. (2004). Formation mechanism of the theta aurora by a transient convection during northward IMF. *Journal of Geophysical Research*, *109*, A09201. https://doi.org/10.1029/2003JA010271

Tanaka, T., Obara, T., Watanabe, M., Fujita, S., Ebihara, Y., & Kataoka, R. (2017). Formation of the Sun-aligned arc region and the void (polar slot) under the null-separator structure. *Journal of Geophysical Research: Space Physics*, *122*, 4102–4116. https://doi.org/10.1002/2016JA023584

Tanaka, T., Obara, T., Watanabe, M., Fujita, S., Ebihara, Y., Kataoka, R., & Den, M. (2018). Cooperatives roles of dynamics and topology in generating the magnetosphere-ionosphere disturbances: Case of the theta aurora. *Journal of Geophysical Research: Space Physics*, *123*, 9991–10,008. https://doi.org/10.1029/2018JA025514

Tanaka, T., Obara, T., Watanabe, M., Fujita, S., Ebihara, Y., Kataoka, R., & Den, M. (2019). Magnetosphere-ionosphere convection under the due northward IMF. *Journal of Geophysical Research: Space Physics*, *124*, 6812–6832. https://doi.org/10.1002/2019JA026547

Tanaka, T., Watanabe, M., Den, M., Fujita, S., Ebihara, Y., Kikuchi, T., et al. (2016). Generation of field-aligned current (FAC) and convection through the formation of pressure regimes: Correction for the concept of Dungey's convection. *Journal of Geophysical Research: Space Physics*, *121*, 8695–8711. https://doi.org/10.1002/2016JA022822

Tsunomura, S. (1999). Numerical analysis of global ionospheric current system including the effect of equatorial enhancement. *Annales de Geophysique*, *17*, 692–706.

Watanabe, M., Tanaka, T., & Fujita, S. (2019). Magnetospheric dynamo driving large-scale Birkeland currents. *Journal of Geophysical Research: Space Physics*, *124*, 4249–4265. https://doi.org/10.1029/2018JA026025

Wilder, F. D., Eriksson, S., & Wiltberger, M. (2015). The role of magnetic flux tube deformation and magnetosheath plasmabeta in the saturation of the Region 1 field-aligned current system. *Journal of Geophysical Research: Space Physics*, *120*, 2036–2051. https://doi.org/10.1002/2014JA020533

Yu, Y., & Ridley, A. J. (2008). Validation of the space weather modeling framework using ground-based magnetometers. *Space Weather*, *6*, S05002. https://doi.org/10.1029/2007SW000345

Yu, Y., Ridley, A. J., Welling, D. T., & Tóth, G. (2010). Including gap region field-aligned currents and magnetospheric currents in the MHD calculation of ground-based magnetic field perturbations. *Journal of Geophysical Research*, *115*, A08207. https://doi.org/10.1029/2009JA014869